

X-Ray Flares In GRB090812 - Case Study

Shlomo Dado¹ and Arnon Dar²

ABSTRACT

The master formulae of the CB model of long durations gamma ray bursts (GRBs) which reproduce very well the light curves and spectral evolution of their prompt emission pulses and their smooth afterglows, also reproduce very well the lightcurves and spectral evolution of their X-ray and optical flares. Here we demonstrate that for GRB090812

1. Introduction

In more than 50% of the gamma ray bursts (GRBs) observed with the Swift X-ray telescope (XRT), flares were observed at the end of the prompt emission and/or the early AG phase (see, e.g., Burrows et al. 2005; Burrows et al. 2007; Falcone et al. 2007). In some cases X-ray flares were observed also at very late times, of the order of several days after the prompt emission. Flares in GRBs were studied phenomenologically by various observer groups (see, e.g., Burrows et al. 2005; Burrows et al. 2007; Kocevski & Butler 2007; Butler & Kocevski 2007; Falcone et al. 2007; Chincarini et al. 2007a,b, 2008a,b, and references therein). Modifications of previously suggested models and new theoretical models were proposed and discussed by several authors but none of the proposed models was shown to actually derive the observed spectral and temporal properties of either early-time flares or late-time flares from underlying physical assumptions except for the cannonball model of GRBs (see, e.g., Dado & Dar, hereafter DD, 2009b and references therein).

Flares are a natural consequence of the cannonball (CB) model of GRBs, which was motivated by a GRB-microquasar analogy (e.g., Dar & De Rújula 2004 and references therein, Dado, Dar & De Rújula, hereafter DDD, 2002; 2009). In the CB model, *long-duration* GRBs and their AGs are produced by bipolar jets of highly relativistic plasmoids of ordinary matter ejected in accretion episodes on the newly formed compact stellar object (Shaviv & Dar

¹dado@phep3.technion.ac.il

Physics Department, Technion, Haifa 32000, Israel

²arnon@physics.technion.ac.il

Physics Department, Technion, Haifa 32000, Israel

1995; Dar 1998) in core-collapse supernova (SN) explosions (Dar et al. 1992; Dar & Plaga 1999). It is hypothesized that an accretion disk or a torus is produced around the newly formed compact object, either by stellar material originally close to the surface of the imploding core and left behind by the explosion-generating outgoing shock, or by more distant stellar matter falling back after its passage (De Rújula 1987). As observed in microquasars, each time part of the accretion disk falls abruptly onto the compact object, two jets of cannonballs (CBs) made of *ordinary-matter plasma* are emitted with large bulk-motion Lorentz factors in opposite directions along the rotation axis wherefrom matter has already fallen back onto the compact object due to lack of rotational support. The prompt γ -ray and X-ray emission is dominated by inverse Compton scattering (ICS) of photons of the SN glory - scattered and/or emitted light by the SN filling the cavity produced by the pre-supernova wind/ejecta which was blown from the progenitor star long before the GRB. The CBs' electrons Compton up-scatter the glory photons into a narrow conical beam of γ rays along the CBs' direction of motion. An X-ray 'flare' coincident in time with a prompt γ -ray pulse is simply its low-energy part. The flares ending the prompt emission and during the early time afterglow is the same: ICS of glory photons by the electrons of CBs ejected in late accretion episodes of fall-back matter on the newly formed central object (e.g., Dar 2006). The early time X-ray flares without an accompanying detectable γ -ray emission are usually IC flares (ICFs) produced by CBs with relatively smaller Lorentz factors: As the accretion material is consumed, the 'engine' has a few progressively-weakening dying pangs. Like the lightcurves of the prompt GRB pulses, the lightcurves of ICFs exhibit a rapid softening during their fast decline phase (see, e.g. Evans et al. 2007,2009). Often, the fast decay of an ICF is taken over by synchrotron radiation (SR) from the CB's encounter with the wind enclosing the glory light before the take over by the plateau/shallow-decay phase of the afterglow (AG).

The initial expansion of the CBs and the slowing-down of the leading ones by the circumburst matter merge most of them during the afterglow phase into a single leading CB (Dar & De Rújula 2004, DDD2009). The prompt emission beam of gamma rays ionizes the matter in front of the CB. The ions continuously impinging on the CB with a relative Lorentz factor $\gamma(t)$, where $\gamma(t)$ is the bulk motion Lorentz factor of the CB, generate within it an equipartition turbulent magnetic field. The intercepted electrons are isotropized and Fermi accelerated by these fields and emit isotropic synchrotron radiation in the CB's rest frame, which is Doppler boosted and beamed relativistically into a narrow cone with a typical opening angle $\sim 1/\gamma(t)$. Late synchrotron radiation flares (SRFs) are produced mainly when the CBs encounter winds or density bumps along their path first from the progenitor star and later in the interstellar medium (ISM). The lightcurve of these flares depends on the unknown density profile of the encountered wind/density bump which cannot be predicted a-priori. But, both the early-time and the late-time SRFs have a typical SR spectrum and

a weak spectral evolution which are quite different from those of the accretion induced ICFs and can be used to identify their origin – late ejection episodes from the central engine or encounters with density bumps.

2. The master formula for ICS flares

Let t denote the time in the observer frame after the beginning of a flare ($t = T - T_i$ where T is the time after trigger and T_i is its value at the beginning of the flare). The light-curve of a flare, produced by the electrons in a CB by ICS of thermal bremsstrahlung photons filling the cavity formed by a wind blown by the progenitor star long before the GRB, is generally well approximated by (DDD2009 and references therein):

$$E \frac{d^2 N_\gamma}{dt dE}(E, t) \approx A \frac{t^2 / \Delta t^2}{(1 + t^2 / \Delta t^2)^2} e^{-E/E_p(t)} \propto e^{-E/E_p(0)} F(E t^2), \quad (1)$$

where A is a constant which depends on the CB's baryon number, Lorentz and Doppler factors, and on the density of the glory light and on the redshift and distance of the GRB, and $E_p(t)$, the peak energy of $E^2 d^2 N_\gamma / dE dt$ at time t is given roughly by:

$$E_p(t) \approx E_p(0) \frac{t_p^2}{t^2 + t_p^2}, \quad (2)$$

with t_p being the time (after the beginning of the flare) when the ICS photon count-rate reaches peak value. For $E \ll E_p$, it satisfies $E_p(t_p) = E_p$ where E_p is the peak energy of the time-integrated spectrum of the flare. Thus, in the CB model, each ICF in the GRB lightcurve is described by four parameters, A , $\Delta t(E)$, $E_p(0)$ and T_i , the beginning time of the pulse when t is taken to be 0.

The late-time decay of the energy flux of the prompt emission pulses and ICFs in an energy band $[E1, E2]$, which follows from Eq. (1), is given approximately by,

$$\int_{E1}^{E2} E \frac{d^2 N_\gamma}{dt dE}(E, t) dE \approx A \frac{E_p(t) \Delta t^2}{t^2} [e^{-E1/E_p(t)} - e^{-E2/E_p(t)}]. \quad (3)$$

Thus, for the Swift XRT lightcurves where $E1 = 0.3$ keV and $E2 = 10$ keV, as long as $E_p(t) \gg E2 \geq E1$, the energy flux in an ICS pulse/flare decays like t^{-2} until it is taken over by the SR afterglow. If $E1 \ll E_p(t)$ but $E2 \gtrsim E_p(t)$ the energy flux decays like t^{-4} , and when $E1 \gtrsim E_p(t)$ the energy flux decays like $t^{-4} e^{-E t^2 / 2 E_p t_p^2}$.

3. The lightcurve of early-time SR flares

The SR radiation which is emitted from the encounter of a CB with the wind/ejecta of the progenitor star with a density profile $n(r) \propto e^{-a_r/(r-r_w)}/(r-r_w)^2$ for $r > r_w$ and $n(r) = 0$ for $r < r_w$ is given approximately by (DDD2009, DD2008):

$$F_\nu \propto \frac{e^{-a/t} t^{1-\beta}}{t^2 + t_{exp}^2} \nu^{-\beta}, \quad (4)$$

where $t = T - T_w$ with T being the time after trigger and T_w the time of the CB-wind encounter, t_{exp} is the typical slow-down time of the fast CB expansion, $\beta = \Gamma - 1$, and the exponent describes the decreasing attenuation of the emitted radiation when the CB penetrates the wind, or more likely, the initial rise in the wind density due to an exponential cutoff in the wind ejection if the observed rise in the prompt SRF is achromatic. (A Gaussian cutoff, e^{-a^2/t^2} , may be required by very sharp achromatic SRFs). Note that for $t^2 \gg t_{exp}^2$, the asymptotic decline of an SRF is a simple power law,

$$F_\nu \propto t^{-\Gamma} \nu^{1-\Gamma}, \quad (5)$$

which distinguishes SRFs from ICFs. This asymptotic decline is insensitive to the exact values of the start time and the width of the SRF.

Note that as long as $E_p(t) \gg E$, the temporal decay of ICS pulses/flares that follows from Eq. (1), i.e., $F_\nu \propto t^{-2}$, is similar to that of X-ray SRFs that follows from Eq. (4) for $\Gamma_X \sim 2$, but their spectral indices differ roughly by one unit ($\Gamma_X \sim 1$ for ICFs).

Generally, each ICS flare is accompanied/followed by an SR flare whose lightcurve is given by Eq. (4). However the SR flares are wider and very often blended and the temporal structure is either smoothed or missed because of low temporal resolution (see, e.g., Figure 1 in Bartolini et al 2009).

4. The canonical SR afterglow

For a constant density ISM and an X-rays well above the cooling frequency of the Fermi accelerated electrons in the CBs, the unabsorbed spectral energy density of their emitted SR is given by (DDD2009 and references therein),

$$F_{ISM}[\nu, t] \propto \gamma(t)^{3-\beta_X} \delta(t)^{3\beta_X+1} \nu^{-\beta_X} \quad (6)$$

where $\delta = 1/\gamma(1 - \beta \cos\theta)$ is its Doppler factor with θ being the angle between the line of sight to the CB and its direction of motion. For $\gamma^2 \gg 1$ and $\theta^2 \ll 1$, $\delta \approx 2\gamma/(1 + \gamma^2\theta^2)$

to an excellent approximation. In the CB model the canonical value of the spectral index above the characteristic frequency has the value $\beta_X \approx 1.1$. For a CB of a baryon number N_B , a radius R and an initial Lorentz factor γ_0 , relativistic energy-momentum conservation yields the deceleration law of the CB in an ISM with a constant density n (DDD2009 and references therein):

$$\gamma(t) = \frac{\gamma_0}{[\sqrt{(1 + \theta^2 \gamma_0^2)^2 + t/t_0} - \theta^2 \gamma_0^2]^{1/2}}, \quad (7)$$

with $t_0 = (1+z) N_B / 8 c n \pi R^2 \gamma_0^3$. As can be seen from Eq. (7), γ and hence δ change little as long as $t \ll t_b = [1 + \gamma_0^2 \theta^2]^2 t_0$, and Eq. (6) yields the ‘plateau’ phase of canonical AGs. For $t \gg t_b$, γ and δ decrease like $t^{-1/4}$. The transition $\gamma(t) \sim \gamma_0 \rightarrow \gamma \sim \gamma_0 (t/t_0)^{-1/4}$ around t_b induces a bend, the so called ‘jet break’, in the synchrotron AG from a plateau to an asymptotic power-law decay,

$$F_{ISM}[\nu, t] \propto t^{-\beta_X - 1/2} \nu^{-\beta_X}. \quad (8)$$

Thus, the shape of the entire lightcurve of the SR afterglow after entering the constant density ISM depends on only three parameters, the product $\gamma_0 \theta$, the deceleration parameter t_0 (or the break time t_b) and the spectral index β_X . The post break decline is given by the simple power-law (Eq. 8) independent of the values of $\gamma_0 \theta$ and t_b . In cases where t_b is earlier than the beginning of the XRT observations or is hidden under the prompt emission, the entire observed lightcurve of the AG has this asymptotic power-law form (DDD2008a).

For a wind density profile, $n \propto 1/r^2$ beyond $r = r_w$, the asymptotic decline is given by

$$F_W[\nu, t] \propto t^{-\beta_X - 1} \nu^{-\beta_X}, \quad (9)$$

where t is the time after the onset of the $n \propto 1/r^2$ density. This relation describes well the asymptotic decay of late-time SRFs (DDD2003; DDD2009).

5. GRB090812

Observations: The Swift Burst Alert Telescope (BAT) triggered and located GRB 090812 on August 12, 2009 at 06:02:08 UT (Stamatikos et al. 2009). The BAT light curve (energy flux in the 15-350 keV range) showed three peaks around 5, 27 and 55 sec, respectively, after trigger (Baumgartner et al. 2009). The total duration of the burst was approximately 70 sec. A joint spectral analysis of the Konus-Wind and Swift/BAT time integrated spectrum in the 23-1400 keV energy band was well fit with a power-law with exponential cutoff with a power-law index -1.03 ± 0.07 and peak energy $E_p = 572(-159, +251)$ keV (Pal’shin et al. 2009). The Swift X-ray telescope (XRT) began observing the field at 06:03:25.7 UT, 76.8

seconds after the BAT trigger. The X-ray lightcurve in the 0.3-10 keV band that was inferred from the Swift XRT observations is shown in Fig. 1a. It was reproduced from the Swift/XRT GRB lightcurve repository (http://www.swift.ac.uk/xrt_curves/, Evans et al. 2007,2009). It shows the X-ray tail of the last pulse detected by the BAT around 55 sec followed by two prominent X-ray flares which are taken over around 600s by a smooth $\sim t^{-2}$ decline until a gap in the data between 1.15 ks and 11.5 ks after which the light curve decay like a post-break power-law $\sim t^{-1.4}$. Inspection of the hardness ratio measured by the XRT and reported in the Swift/XRT GRB lightcurve repository reveals the typical fast decay of flares ending the prompt emission that is accompanied by a rapid spectral softening. The fast falling hardness ratio increases back to a constant value around 600 sec and remains so during the rest of the afterglow observations with the XRT. The constant photon spectral index during this phase is (Swift/XRT GRB lightcurve Repository): $\Gamma_X=1.914 (+0.138, -0.089)$.

The optical AG of GRB090812 was first detected 24 s after the BAT trigger by the RAPTOR telescope (Wren et al. 2009). A redshift $z=2.542$ was inferred for GRB 090812 from early-time observations using the FORS2 at the VLT (de Ugarte Postigo et al. 2009). Its optical AG was also detected and followed-up by the Swift UVO telescope (Stamatikos et al. 2009; Schady et al. 2009), the automated Palomar 60 inch telescope (Cenko et al. 2009), the 2 m Liverpool automated Telescope (Smith et al. 2009), the 2.2 m ESO/MPI telescope (Utdike et al. 2009), and the Faulkes Telescope South (Cano et al. 2009). The R-band light curve from these GCN reports is shown in Fig 2. It reveals a brightening AG until ~ 70 s after the trigger that turned into a power-law decay. Such behaviour is typical of the prompt optical emission detected with robotic telescopes, by now in many bright GRBs (see, e.g., Fig. 3) such as 090123 (Akerlof et al. 1999), 030418 (Rykoff et al. 2004), 050820A (Cenko et al 2006), 060418 (Molinari et al. 2007), 060605 (Ferrero et al. 2009), 060607A (Molinari et al. 2007; Ziaeeepour et al. 2008; Covino et al. 2008a; Nysewander et al. 2009), 061007 (Mundell et al. 2007), 071010A (Covino et al. 2008b) 081203A, (Kuin et al. 2009), 090102 (Klotz et al. 2009a,b; Covino et al. 2009), and 090618 (Li et al. 2009).

CB model interpretation of the XRT lightcurve: The spectral evolution of the X-ray tail of the last flare detected by the Swift BAT around 55 sec and of the following two X-ray flares detected by the Swift XRT are that expected in the CB model for ICFs (DDD2009, DD2009b). Consequently, we have reproduced the early-time XRT lightcurve by a sum of an X-ray tail and two prominent ICFs (Eq. (1)) which is taken over by the tails of the SRFs (Eq. (4)) that are associated with these ICFs. The late time X-ray afterglow was reproduced by a CB model post-break SR afterglow, as given by Eqs. (6) and (7). The values of the parameters used in the CB model description of the complete X-ray lightcurve are listed in Table 1. Because of the approximations, the possibility of local minima in the χ^2 search and degeneracy of parameters, the best fit values of the parameters, probably are effective

(approximate) values and are not necessarily their exact physical values. For instance, the tail of the first ICF is not sensitive to its beginning time and its width. The joint tail of the SRFs depends only on β_X . The spectral index parameter p in the description of the AG was constrained to satisfy the CB model closure relation for GRB090812: $p/2 = \beta_x = \Gamma_X - 1 = 0.914$ (+0.138, -0.089). However, because of the gap in the XRT data between 1.15 ks and 11.5 ks and the large uncertainty in the value of β_X inferred from the data, the values of p , $\gamma_0\theta$ are not well determined by the fit. Thus, in the CB-model description of the late-time X-ray AG we adopted the central value reported in the Swift/XRT GRB lightcurve repository, $\beta_X = 0.914$, which yields a post-break behaviour, $F_\nu \propto t^{-1.43}$ and the best fit values $\gamma_0\theta = 1.34$ and $t_b = 598$ sec. The CB-model description of the complete XRT lightcurve is shown in Fig. 1a. An enlarged view of the early time behaviour is shown in Fig. 1b. This CB model description yields $\chi^2/dof = 481/421 = 1.18$.

CB model interpretation of the optical lightcurve: The data on the optical lightcurve of GRB090812 that was reported by different groups in GCN reports are preliminary, sparse, was neither cross calibrated nor corrected for extinction along the whole line of sight. Despite that, the data show roughly the behaviour predicted by the CB model, which is demonstrated in Fig. 2. The CB model description assumes a prompt emission SRF from the encounter of the CBs with the wind/ejecta blown by the progenitor star long before the GRB, which begins in the observer frame towards the end of the first γ -ray flare detected by the Swift BAT, and turns into a power-law decline (Eq. 4) that is taken over by the achromatic SR afterglow ($\beta_O = \beta_X$, $\gamma_0\theta = 1.34$ and $t_b = 598$ sec obtained from the CB-model fit to the X-ray AG). The broad SRF is probably dominated by a sum of 3 unresolved SRFs associated with the 3 prominent BAT flares. and the 2 prominent XRT flares which are blended together into a broad SRF. The effective parameters which were used in the CB-model description of the prompt emission SRF are $t_0 \sim 10$ sec, $t_{exp} \sim 66$ sec, $a \sim 21.3$ sec and $\beta_O \sim 0.55$. Only in very bright GRBs, such as 080319B the prompt optical emission is resolved into separate SRFs (Racusin et al. 2008), associated with the prompt γ -ray flares, as shown in Fig. 2b borrowed from DD2008.

Conclusion: The lightcurves and spectral evolution of the X-ray and optical flares in GRB090812 are well reproduced by the CB model.

REFERENCES

- Akerlof, C., et al. 1999, Nature, 398, 400
 Bartolini, C., et al. 2009, arXiv:0906.4144

- Baumgartner, W., et al. 2009, GCN Circ. 9775
- Burrows, D. N., et al. 2005, *Science*, 1833, 2005
- Burrows, D.N., et al. 2007, *MNRAS*, 365, 1213, 2007
- Butler, N. & Kocevski, D. 2007, *ApJ*, 663, 407
- Cano, Z., et al. 2009, GCN Circ. 9779
- Cenko, S.B., et al. 2006, *ApJ*, 652, 490
- Cenko, S.B., et al. 2009, GCN Circ. 9769
- Chincarini, G., et al. 2007a, *AdSpR*, 40, 1199
- Chincarini, G., et al. 2007b, *ApJ*, 671, 1903
- Chincarini, G., et al. 2008a, arXiv:0809.1026
- Chincarini, G., et al. 2008b, arXiv:0809.2151
- Covino, S., et al. 2008a, *MNRAS*, 388, 347
- Covino, S., et al. 2008b, *ChJAS*, 8, 356
- Covino, S., et al. 2009, GCN Circ. 8963
- Dado, S. & Dar, A. 2008, arXiv:0812.3340 (DD2008)
- Dado, S. & Dar, A. 2009a, *AIP Conf. Proc.* 1111, 333 (DD2009a)
- Dado, S. & Dar, A. 2009b, arXiv:0908.0650 (DD2009b)
- Dado, S., Dar, A. & De Rújula, A. 2002, *A&A*, 388, 1079 (DDD2002)
- Dado, S., Dar, A. & De Rújula, A. 2008a, *ApJ*, 680, 517 (DDD2008a)
- Dado, S., Dar, A. & De Rújula, A. 2008b, *ApJ*, 681, 1408 (DDD2008b)
- Dado, S., Dar, A. & De Rújula, A. 2009, *ApJ*, 696, 994 (DDD2009)
- Dar, A., et al. 1992, *ApJ*, 388, 164
- Dar, A. 1998, *ApJ*, 500, L93
- Dar, A. 2006, *ChJAS*, 6, 301 (arXiv:astro-ph/0511622)

- Dar, A. & De Rújula, A. 2004, *Phys. Rep.* 405, 203
- Dar, A. & Plaga, R. 1999, *A&A*, 349, 259
- De Rújula, A. 1987, *Phys. Lett.* 193, 514
- de Ugarte Postigo, A., et al. 2009, *GCN Circ.* 9771
- Evans, P., et al. 2007, *A&A*, 469, 379.
- Evans et al. 2009, *MNRAS*, submitted (arXiv:0812.3662)
- Falcone, A., et al., *ApJ*, 641, 1010 (2006)
- Falcone, A., et al., *ApJ*, 671, 1921 (2007)
- Ferrero, P., et al. 2009, *A&A*, 497, 729
- Klotz, A., et al 2009a, *GCN Circ.* 8761
- Klotz, A., et al 2009b, *GCN Circ.* 8764
- Kocevski, D., & Butler, N., 2007, *ApJ*, 667, 1024
- Kuin, N. P. M., et al. 2009, *MNRAS*, 395, L21
- Li, W., et al. 2009, *GCN Circ.* 9517
- Molinari, E., et al. 2007 *A&A*, 469, L13
- Mundell, C. G., et al. 2007, *ApJ*, 660, 489
- Nysewander, M., et al. 2009, *ApJ*, 693, 1417
- Pal'shin, V., et al. 2009, *GCN Circ.* 9821
- Racusin, J. L., et al. 2008, *Nature*, 455, 183
- Rykoff, E.S., et al. 2004, *ApJ*, 601, 1013
- Schady, P., et al. 2009, *GCN Circ.* 9774
- Shaviv, N. J. & Dar, A. 1995, *ApJ*, 447, 863
- Smith, R. J., et al. 2009, *GCN Circ.* 9770
- Stamatikos, M., et al. 2009, *GCN Circ.* 9768

Updike, A., et al. 2009, GCN Circ. 9773

Wren, J., et al. 2009, GCN Circ. 9778

Ziaeeepour, H., et al. 2008, MNRAS, 385, 453

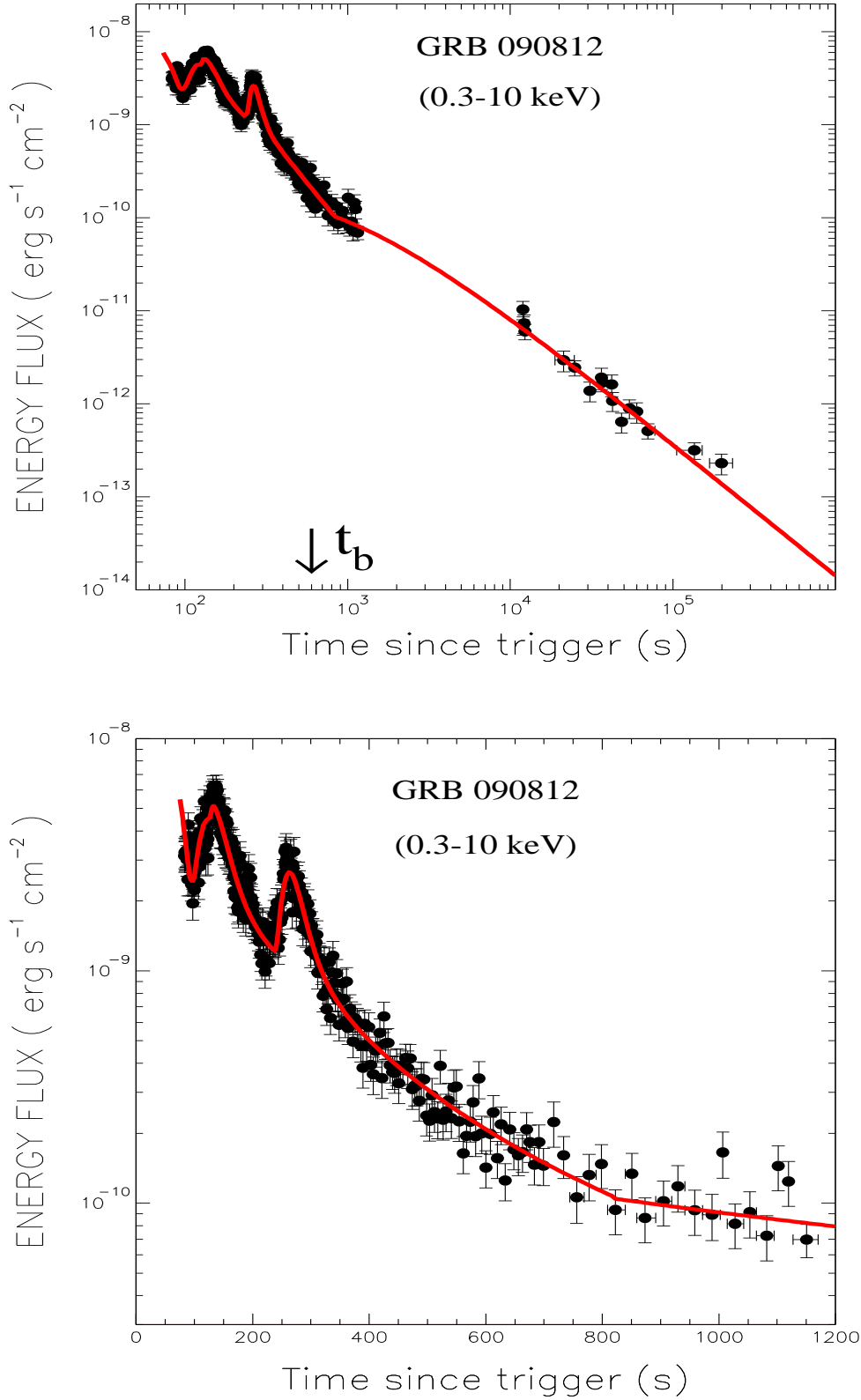


Fig. 1.— **Top (a)**: Comparison between the 0.3-10 KeV X-ray lightcurve of GRB090812 measured with the Swift XRT and reported in the Swift/XRT lightcurve repository http://www.swift.ac.uk/xrt_curves/ (Evans et al. 2009) and its CB model description as detailed in the text. **Bottom (b)**: Enlarged view of the comparison in part (a) for the early time flares.

Table 1. The parameters of the ICFs used in the CB model description of X-ray lightcurves of Swift GRBs.

| flare | t_i [s] | Δt | $E_p(0)$ [keV] | A [erg/cm ² s ⁻¹] |
|-------|------------------|------------|----------------|--|
| ICF1 | 40.3 | 25.6 | 9.76 | 0.26^{-7} |
| ICF2 | 90.4 | 54.3 | 0.45 | 0.23^{-6} |
| ICF3 | 236.8 | 35.4 | 4.30 | 0.80^{-8} |
| SRF | t_i [s] | t_{exp} | a [s] | |
| — | 125.4 | 165.4 | 2.0 | |
| AG | $\gamma_0\theta$ | t_0 [s] | β_X | |
| | 1.095 | 182 | 0.98 | |

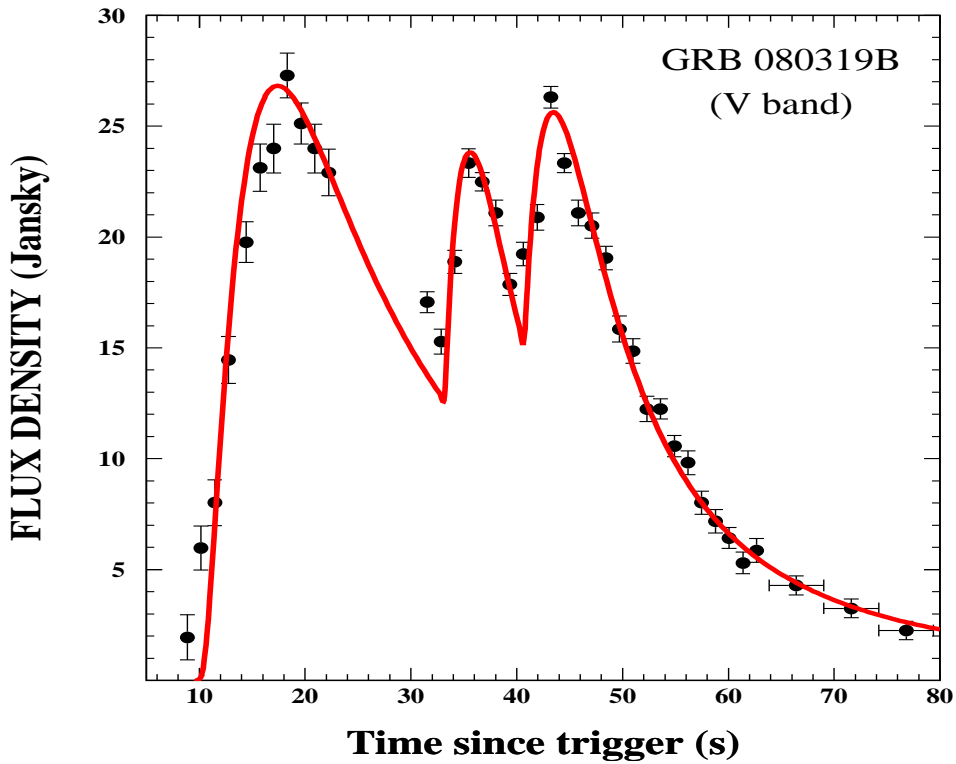
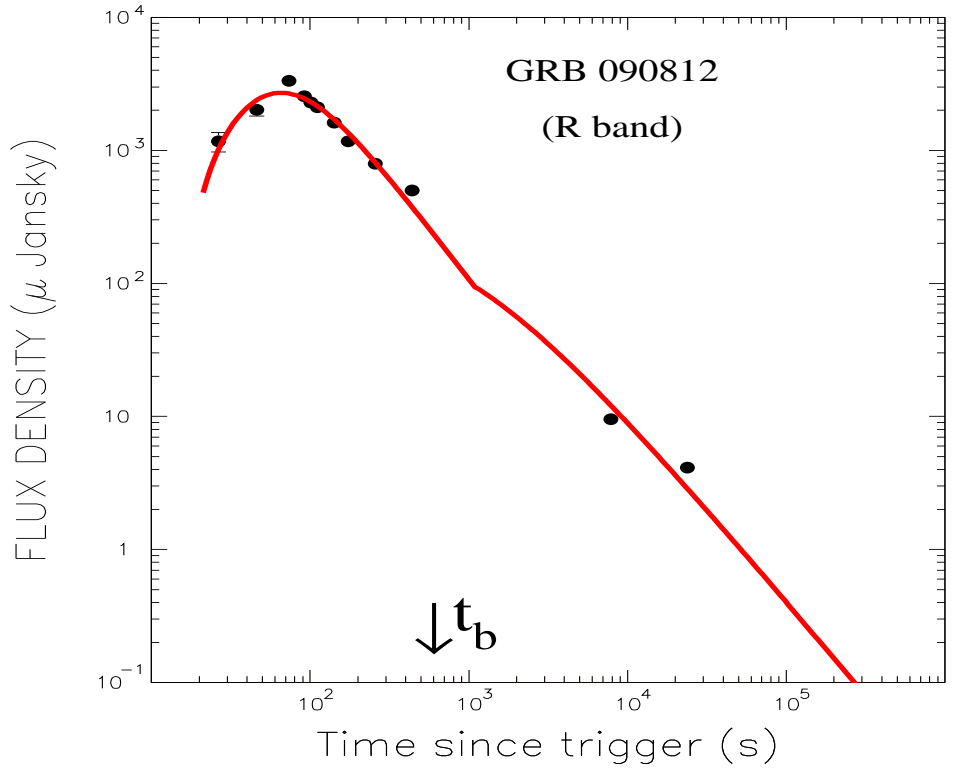


Fig. 2.— **Top (a):** Comparison between the R -band lightcurve of the prompt optical emission in the bright GRB 090812 and its CB model description as detailed in the text. **Bottom (b):** Comparison between the V -band lightcurve of the prompt optical emission in GRB080319B, the brightest observed GRB so far, and its CB model description as detailed in DD2008. The smooth lightcurve of GRB090812, in contrast to that of GRB080319B, may result from low temporal resolution due to low statistics and/or due to blending of the individual optical flares following/associated with its prompt emission.

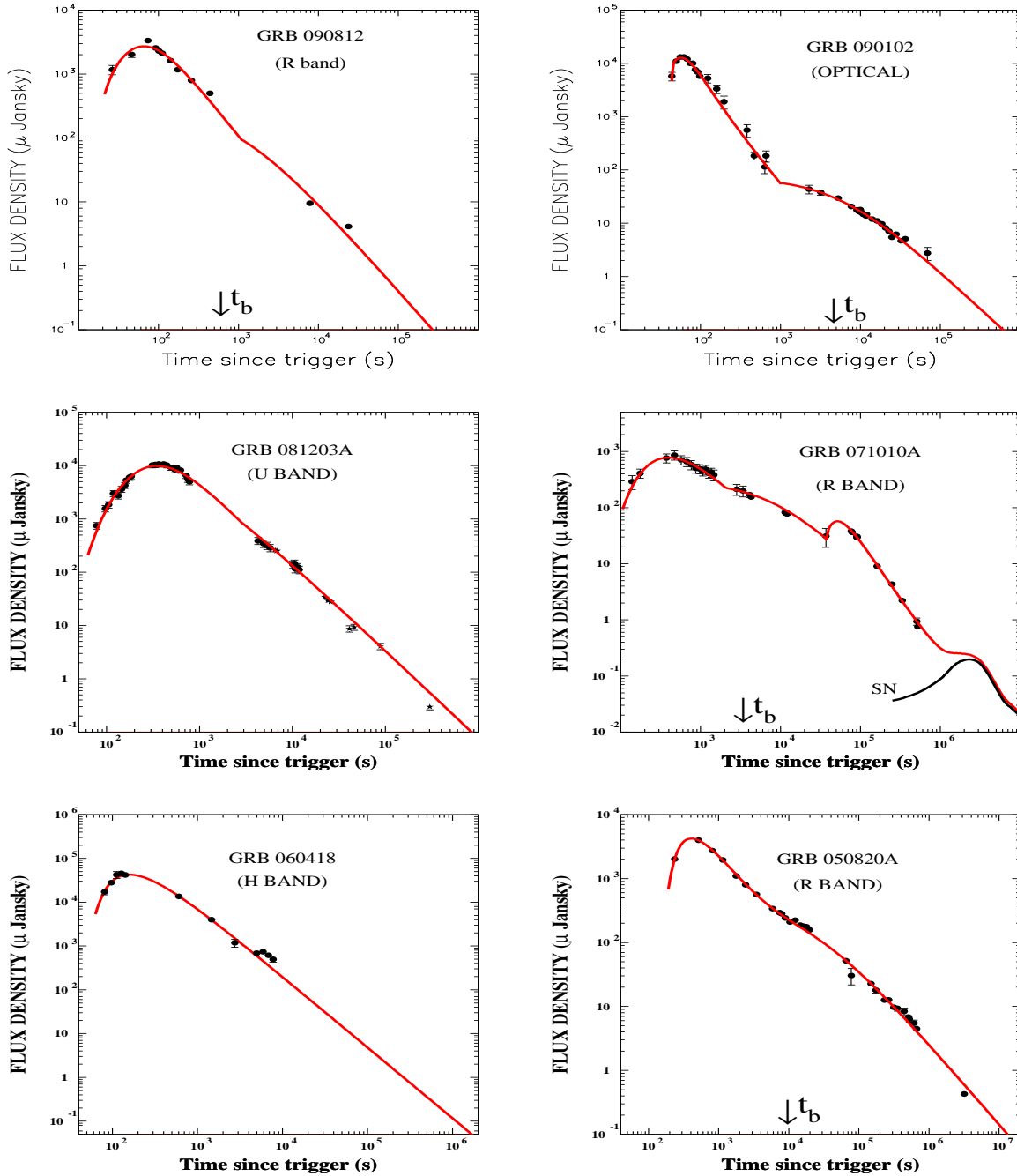


Fig. 3.— The R-band lightcurve of GRB090812 and a few similar optical lightcurves of other GRBs which were detected by automated telescopes during the prompt emission phase of these GRBs. Also shown is their CB-model description (with exponential cutoffs of wind ejections). **Top left (a):** GRB 090812. See text for details. **Top right (b):** GRB 090102. Figure borrowed from DD2009a. **Middle left (c):** GRB 081203A. Figure borrowed from DD2009a. **Middle right (d):** GRB 071010A. Figure borrowed from DDD2009. **Bottom left (e):** GRB 060418. Figure borrowed from DDD2009. **Bottom right (f):** GRB 050820A. Figure borrowed from DDD2009.